

Synthesis and Characterization of $\text{La}_{0.8}\text{Sr}_{0.2}\text{MnO}_{3-\delta}$ Nanostructures for Solid Oxide Fuel Cells

V. S. Reddy Channu^{1*}, Rudolf Holze¹, Edwin H. Walker²

¹Institut für Chemie, AG Elektrochemie, Technische Universität Chemnitz, Chemnitz, Germany; ²Department of Chemistry, Southern University and A&M College, Baton Rouge, USA.

Email: *chinares02@gmail.com

Received October 15th, 2012; revised November 15th, 2012; accepted November 25th, 2012

ABSTRACT

$\text{La}_{0.8}\text{Sr}_{0.2}\text{MnO}_{3-\delta}$ (LSM) perovskite was synthesized using different methods, such as solid state reaction, soft-chemical and sol-gel methods for solid oxide fuel cells (SOFCs) for use as a cathode material. The pristine material was characterized by X-ray diffraction, thermogravimetric analysis (TGA), differential scanning calorimetry (DSC) and scanning electron microscopy (SEM). X-ray diffraction results show that the pure phase of $\text{La}_{0.8}\text{Sr}_{0.2}\text{MnO}_{3-\delta}$ (LSM) perovskite was formed at 1250°C. Scanning electron microscopy characterization shows that a highly porous material can be obtained using a soft-chemical method with different 3,3',3''-nitrotripropionic acid (NTP) to metal-ion ratio *R*.

Keywords: Porous Materials; Characterization Techniques; Cathode

1. Introduction

Perovskite $\text{La}_{1-x}\text{Sr}_x\text{MnO}_3$ (LSMO) has attracted attention because of its potential applications in magnetic sensors, reading heads for magnetic memories and as a cathode in solid oxide fuel cells (SOFCs) due to its excellent catalytic, thermal, electrical and magnetic properties [1-4]. The cathode is one of the most essential components in a SOFC. The cathode materials for SOFCs have to meet several requirements in the operating temperature up to 800°C - 1000°C: high electronic conductivity, resistance to sintering, thermal and chemical stability, high catalytic activity for oxygen reduction and a thermal expansion coefficient matching with other SOFC components [5]. Strontium doped lanthanum manganite (LSM, $\text{La}_{1-x}\text{Sr}_x\text{MnO}_3$) is the most frequently used cathode material for zirconia based SOFCs. It is a perovskite material with intrinsic *p*-type conductivity and can meet these requirements. The *p*-type conductivity of LaMnO_3 is a result of the formation of cation vacancies and is enhanced by substituting with a lower valence ion as a dopant such as the alkaline earth in A and/or B sites. The LSM with the typical composition $\text{La}_{0.8}\text{Sr}_{0.2}\text{MnO}_{3-\delta}$ is broadly established as the cathode material for high temperature SOFCs. The particle size and microstructure of electrode are significant for the electrode performance. Several preparation techniques such as solid state reaction, gelcasting, drip pyrolysis, citrate-gel process, solgel process, hydrothermal, co-precipitation, pulse laser deposition, magnetron

sputtering, molecular beam epitaxy, electrochemical deposition and aerosol pyrolysis methods are used to prepare LSM powders and films [6-17]. For the SOFCs application, homogeneous nanosized and high purity powders are required. The LSM powders prepared by the solution chemistry methods regularly have smaller particle size than the solid state reaction method. The solid state reaction method influences the catalytic activity because the temperature during synthesis is too high. A poor surface area of LSM particles results from drip pyrolysis. Via the citrate-gel, sol-gel process and coprecipitation routes particle smaller sizes can be synthesized but also the powders frequently aggregate easily. The aim of this work is to find a suitable method to synthesis porous LSM powders.

2. Experimental

2.1. Solid State Reaction

1.688 g of lanthanum oxide (La_2O_3), 0.382 g of strontium carbonate (SrCO_3) and 1.0225 g of manganese oxide (Mn_2O_3) were mixed together in a ball milling unit for 3 h and pressed into pellets. The pellets were fired at 1000°C for 24 h, regrinded, pressed into pellets again and fired at 900°C and 1250°C for 24 h.

2.2. Sol-Gel Method

3.37 g of lanthanum nitrate ($\text{La}(\text{NO}_3)_3$), 0.55 g of strontium nitrate ($\text{Sr}(\text{NO}_3)_2$) and 2.32 g of manganese nitrate

*Corresponding author.

($\text{Mn}(\text{NO}_3)_2$) were slowly dissolved in 75 mL distilled water. A transparent solution was formed after complete dissolution of the metal nitrates. A gel was formed under continuous stirring and mild heating at 90°C . The gel was dried at 120°C overnight and then heated at 400°C for 12 h. The resulting powders were ground in an agate mortar and heated in air at 1250°C for 12 h in a furnace.

2.3. Soft-Chemical Method

3,3',3''-Nitrilotripropionic acid (NTP) was synthesized using a green chemical method [18]. 3.37 g of lanthanum nitrate ($\text{La}(\text{NO}_3)_3$), 0.55 g of strontium nitrate ($\text{Sr}(\text{NO}_3)_2$) and 2.32 g of manganese nitrate ($\text{Mn}(\text{NO}_3)_2$) were slowly dissolved in 75 mL distilled water. A transparent solution was formed after complete dissolution of the metal nitrates. NTP was dissolved (for different values of the molar NTP to metal-ion ratio R ($R = 0, 0.25, 0.5$ and 0.75) in 100 mL of distilled water at 100°C . This solution was added into the above mentioned transparent solution. The mixed solution was transferred into a 500 mL round-bottom flask and kept at 80°C on a hot plate for 2h to evaporate the solution. A bulky gel of high viscosity was obtained after slowly evaporizing the solution at 80°C by rotary evaporation. The obtained gel was heat treated at 120°C for 24 h in oven. The final product was then ground and made pellets to fire at 400°C and 1250°C for 12 h in furnace.

Crystallographic information on the samples was obtained using an X-ray powder diffractometer (D8 Advanced Bruker) with graphite-monochromatized $\text{CuK}\alpha$ radiation ($\lambda = 1.54187 \text{ \AA}$). Diffraction data were collected over the 2θ range 20° to 80° . The morphologies of the resulting products were characterized using a scanning electron microscope (SEM, JEOL JSM 6390). For the TGA measurements a TA 600, operating in dynamic mode (heating rate = $5^\circ\text{C}/\text{min}$), was employed.

3. Results and Discussion

Phase purity and crystallographic information of the synthesized $\text{La}_{0.8}\text{Sr}_{0.2}\text{MnO}_{3-\delta}$ perovskite nanostructures were characterized using powder X-ray diffraction. The XRD patterns of LSM perovskite nanostructures synthesized by three methods are shown in **Figure 1**. All diffraction patterns of $\text{La}_{0.8}\text{Sr}_{0.2}\text{MnO}_{3-\delta}$ perovskite nanostructures show characteristic peaks of the perovskite phase. The XRD patterns are in good agreement with the standard data for hexagonal symmetry with $a = 5.5163 \text{ \AA}$ and $c = 13.329 \text{ \AA}$ (JCPDS # 00-056-0616). No second phases were observed presumably because a pure phase of $\text{La}_{0.8}\text{Sr}_{0.2}\text{MnO}_{3-\delta}$ (LSM) perovskite was formed at 1250°C [19].

In the synthesis of $\text{La}_{0.8}\text{Sr}_{0.2}\text{MnO}_{3-\delta}$ (LSM) perovskite nanostructures the carrier (3,3',3''-nitrilotripropionic acid

(NTP)) helped in obtaining a homogeneous mixture of the cations in solution through forming metal complexes, it also helped in the reduction of nitrates in a combustion process, releasing a large amount of heat. This is shown by an exothermic peak at 400°C on a DSC curve (**Figure 2**). During the solid-state reduction process, metal cations and oxygen anions stay in the reaction mixture during the formation of the perovskite phase in this combustion process. The large heat released during combustion might help to overcome the lattice energy, which is required for the formation of the perovskite phase, and also in the completion of the nucleation by the rearrangement of atoms by short distance diffusion. The fast combustion process might not be of help for the diffusion of atoms far from each other and hence the particle size of LSM powder remained in the nanometer range.

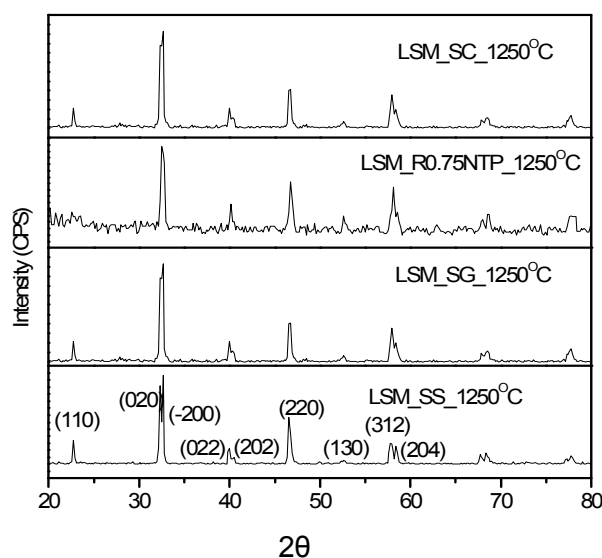


Figure 1. XRD patterns of $\text{La}_{0.8}\text{Sr}_{0.2}\text{MnO}_3$ (LSM) perovskite phase nanoparticles synthesized by different methods.

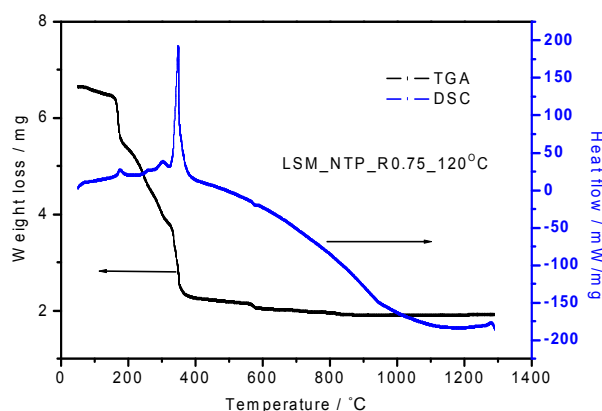


Figure 2. TGA-DSC curves of $\text{La}_{0.8}\text{Sr}_{0.2}\text{MnO}_3$ (LSM) perovskite gel precursor dried at 120°C synthesized by soft-chemical method.

Thermogravimetric analysis and differential scanning calorimetry (TGA-DSC) curves with NTP-assisted LSM dried as a gel at 120°C are shown in **Figure 2**. The weight losses happened in three steps. The total weight loss was 4.75 mg from room temperature to 1300°C . The first weight loss is 0.26 mg in the temperature range 22°C - 157°C ; this can be attributed to evaporation of water from the layers of LSM.

The second weight loss is 3.97 mg in the temperature range 157°C - 357°C and the third weight loss is 0.55 mg in the temperature range 357°C - 840°C . The second and third weight losses are attributed to decomposition of the carrier (NTP) and evaporation of structurally bounded water. The peaks located at about 380°C and 400°C are exothermic on the DSC curve due to decomposition of nitrates and organic matter and correspond to the second weight loss of 3.97 mg from about 157°C to 400°C as observed in the TGA curve. The decomposition of all nitrates is finished below 400°C , which promotes formation of the complex oxides. Here NTP played two roles: One is to form the metal ion complexes and secondly, it serves as a fuel for the combustion reaction, while the nitrates act as an oxidant, so the decomposition reactions can be finished at lower temperatures.

DSC-TGA curves of LSM gel synthesized at 120°C by sol-gel and soft-chemical methods without using chelating agents are shown in **Figures 3** and **4**. The total weight losses are 3.43 mg and 7.02 mg for the sol-gel and soft-chemical method materials from room temperature to 1300°C in three steps. The first weight losses are 0.96 mg and 1.37 mg, they can be attributed to evaporation of water. The second weight losses are 2.44 mg and 4 mg, these correspond to decomposition of the nitrates. The third weight losses are 0.36 mg and 1.65 mg due to evaporation of structurally bounded water. The highest decomposition temperature is about 600°C in both SG and SC methods, which is due to the presence of strontium nitrate.

Figure 5 shows a SEM image of LSM microstructures prepared by solid state (SS) reaction at 1250°C . It shows, that the powder-like material consists of irregular micro-slabs of several micrometers in length. A SEM image of LSM nanoparticles synthesized by sol-gel (SG) method is shown in **Figure 6**. The particle size distribution is more uniform and the size of the particle is about 300 nm - 400 nm. **Figure 7** exhibits scanning electron Microscopy (SEM) images of LSM nanoparticles prepared by soft-chemical method at different NTP to metalion ratios R during the soft-chemical synthesis. LSM particles synthesized without NTP ($R = 0$) show formation of smaller particles with uniform size distribution and the size of the particles about 200 nm - 300 nm (**Figure 7(a)**). LSM particles synthesized using NTP at different R values shows the formation of network nanostructures with

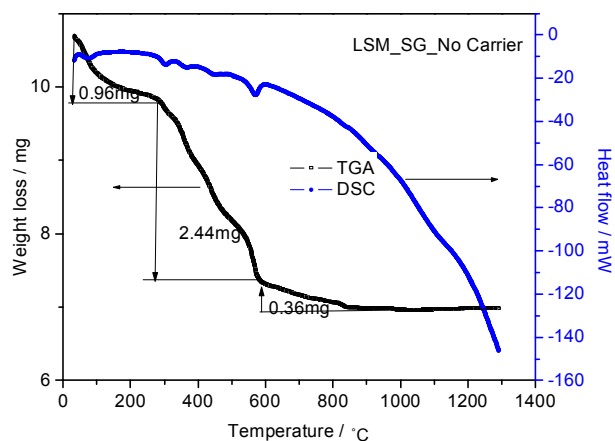


Figure 3. TGA-DSC curves of $\text{La}_{0.8}\text{Sr}_{0.2}\text{MnO}_3$ (LSM) perovskite gel precursor dried at 120°C synthesized by sol-gel method.

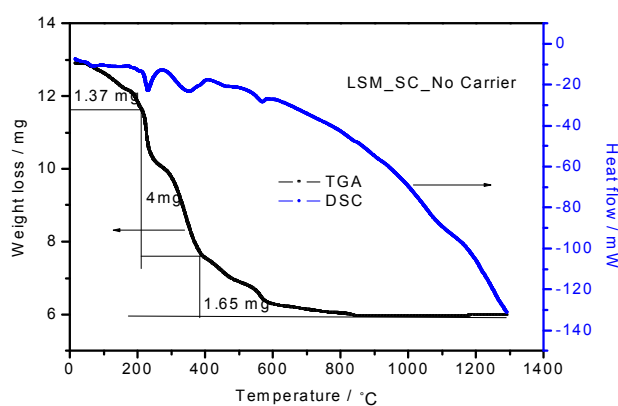


Figure 4. TGA-DSC curves of $\text{La}_{0.8}\text{Sr}_{0.2}\text{MnO}_3$ (LSM) perovskite gel precursor dried at 120°C synthesized by soft-chemical method without NTP.

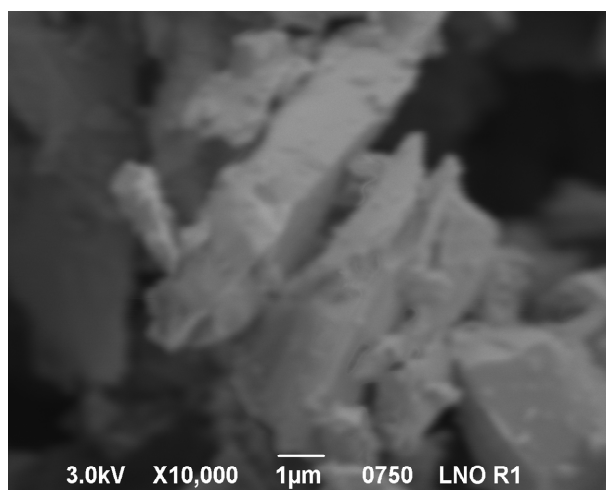


Figure 5. SEM image of LSM micro slabs synthesized by solid state reaction.

higher porosity (**Figures 7(b)-(d)**) contrast to those methods SS, SG and SC without NTP.

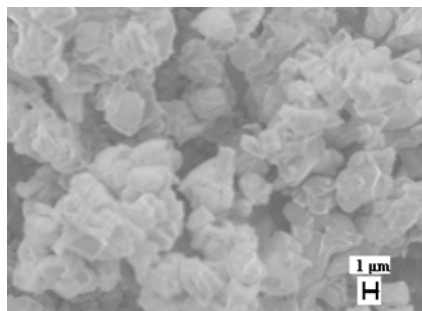


Figure 6. SEM image of LSM nanoparticles prepared by SG method.

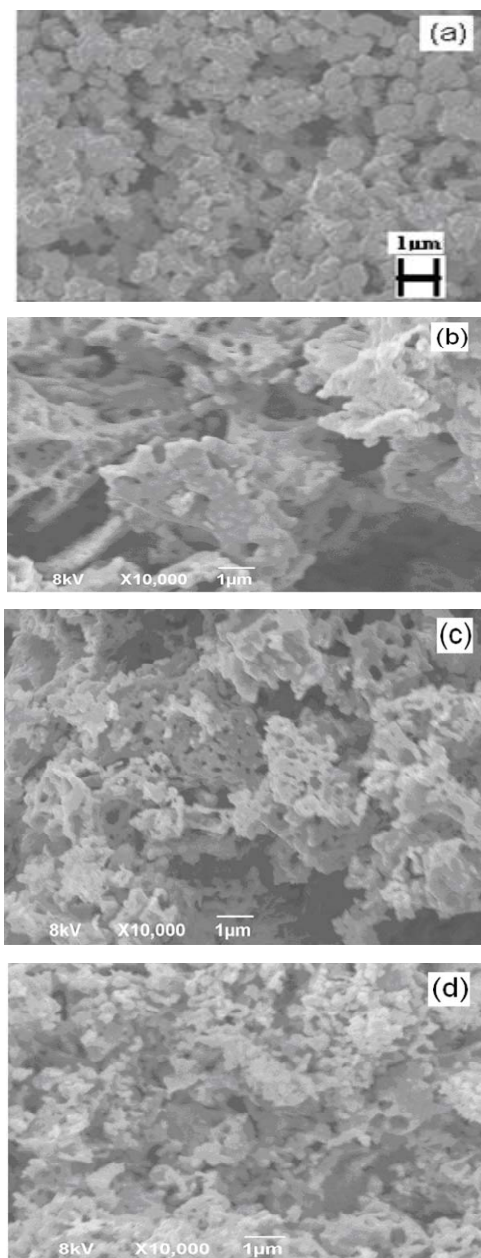


Figure 7. SEM images of LSM synthesized by softchemical method (a) $R = 0$; (b) $R = 0.25$; (c) $R = 0.5$; (d) $R = 0.75$.

4. Conclusion

LSM nanostructures were successfully synthesized by sol-gel and soft-chemical methods. Pure phase perovskite LSM is formed at 1250°C . The decomposition temperature where LSM is obtained is higher in SG and SC methods without NTP when compared to the NTP-assisted SC method. With the latter method highly porous materials were obtained at various 3,3',3"-nitrotripropionic acid (NTP) to metalion ratios.

5. Acknowledgments

One of the authors (V. S. Reddy Channu) thanks the Alexander von Humboldt Foundation for a fellowship.

REFERENCES

- [1] A. J. Upendra and J. S. Lee, "Hydrothermal Synthesis, Characterization and Electrocatalytic Activity of $\text{La}_{0.8}\text{Sr}_{0.2}\text{MnO}_3$ Nanocubes for Oxygen Reduction Reaction," *Solid State Phenomena*, Vol. 119, 2007, pp. 275-278. doi:10.4028/www.scientific.net/SSP.119.275
- [2] T. Tsuchiya, T. Yoshitake, Y. Shimakawa, Y. Kubo, Y. Yamaguchi, T. Manabe, T. Kumagai and S. Mizuta, "Preparation and Characterization of $\text{La}_{0.8}\text{Sr}_{0.2}\text{MnO}_3$ Thin Films by an Excimer Laser MOD Process for a Bolometer," *Applied Physics A Materials Science & Processing*, Vol. 79, No. 4-6, 2004, pp. 1537-1539. doi:10.1007/s00339-004-2842-4
- [3] A. J. Darbandi, T. Enz and H. Hahn, "Synthesis and Characterization of Nanoparticulate Films for Intermediate Temperature Solid Oxide Fuel Cells," *Solid State Ionics*, Vol. 180, No. 4-5, 2009, pp. 424-430. doi:10.1016/j.ssi.2009.01.004
- [4] M. Izumi, Y. Murakami, Y. Konishi, T. Manako, M. Kawasaki and Y. Tokura, "Structure Characterization and Magnetic Properties of Oxide Superlattices $\text{La}_{0.6}\text{Sr}_{0.4}\text{MnO}_3/\text{La}_{0.6}\text{Sr}_{0.4}\text{FeO}_3$," *Physical Review B*, Vol. 60, No. 20, 1999, pp. 1211-1215. doi:10.1103/PhysRevB.60.1211
- [5] J. H. Choi, J. H. Jang, J. H. Ryu and S. M. Oh, "Microstructure and Cathodic Performance of $\text{La}_{0.9}\text{Sr}_{0.1}\text{MnO}_3$ Electrodes According to Particle Size of Starting Powder," *Journal of Power Sources*, Vol. 87, No. 1-2, 2000, pp. 92-100. doi:10.1016/S0378-7753(99)00365-1
- [6] P. Jinhua, S. Kening, Z. Naiqing, X. Shen and Z. Derui, "Preparation and Characterization of $\text{La}_{0.8}\text{Sr}_{0.2}\text{MnO}_{3-\delta}$ Cathode for SOFCs Fabricated Using Azeotropic Distillation Method," *Journal of Rare Earths*, Vol. 24, No. S1, 2006, pp. 93-97. doi:10.1016/S1002-0721(07)60332-9
- [7] L. Zhang, Y. Zhang, Y. D. Zhen and S. P. Jiang, "Lanthanum Strontium Manganite Powders Synthesized Gel-Casting for Solid Oxide Fuel-Cell Cathode Materials," *Journal of American Ceramic Society*, Vol. 90, No. 5, 2007, pp. 1406-1411. doi:10.1111/j.1551-2916.2007.01568.x
- [8] P. Gordes, N. Christiansen, E. J. Jensen and J. Villadsen,

- “Synthesis of Perovskite-Type Compounds by Drip Pyrolysis,” *Journal of Materials Science*, Vol. 30, No. 4, 1995, pp. 1053-1058. [doi:10.1007/BF01178444](https://doi.org/10.1007/BF01178444)
- [9] R. J. Bell, G. J. Millar and J. Drennan, “Influence of Synthesis Route on the Catalytic Properties of $\text{La}_{1-x}\text{Sr}_x\text{MnO}_3$,” *Solid State Ionics*, Vol.131, No. 3-4, 2000, pp. 211-220. [doi:10.1016/S0167-2738\(00\)00668-8](https://doi.org/10.1016/S0167-2738(00)00668-8)
- [10] C. N. Chervin, B. J. Clapsaddle, H. W. Chiu, A. E. Gash, J. H. Jr. Satcher and S. M. Kauzlarich, “A Non-Alkoxide Sol-Gel Method for the Preparation of Homogeneous Nanocrystalline Powders of $\text{La}_{0.85}\text{Sr}_{0.15}\text{MnO}_3$,” *Chemistry of Materials*, Vol. 18, No. 7, 2006, pp. 1928-1937. [doi:10.1021/cm052301j](https://doi.org/10.1021/cm052301j)
- [11] D. Wang, R. B. Yu, S. H. Feng, W. J. Zheng, G. S. Pang and H. Zhao, “Hydrothermal Synthesis of a Giant Magnetoresistance Material $\text{La}_{0.5}\text{Ba}_{0.5}\text{MnO}_3$ under Mild Conditions”, *Chemical Journal Chinese Universities*, Vol. 19, No. 2, 1998, pp. 165-168.
- [12] G. Pang, X. Xu, V. Markovich, S. Avivi, O. Palchik, Y. Koltypin, G. Gorodetsky, Y. Yeshurun, H. P. Buchkremer and A. Gedanken, “Preparation of $\text{La}_{1-x}\text{Sr}_x\text{MnO}_3$ Nanoparticles by Sonication-Assisted Coprecipitation,” *Materials Research Bulletin*, Vol. 38, No. 1, 2003, pp. 11-16. [doi:10.1016/S0025-5408\(02\)01002-4](https://doi.org/10.1016/S0025-5408(02)01002-4)
- [13] E. Koep, C. Jin, M. Haluska, R. Das, R. Narayan, K. Sandhage, R. Snyder and M. Liu, “Microstructure and Electrochemical Properties of Cathode Materials for Sofcs Prepared via Pulsed Laser Deposition,” *Journal of Power Sources*, Vol. 161, No. 1, 2006, pp. 250-255. [doi:10.1016/j.jpowsour.2006.03.060](https://doi.org/10.1016/j.jpowsour.2006.03.060)
- [14] E. S. Vlahov, R. A. Chakalov, R. I. Chakalov, K. A. Nenkov, K. Dorr, A. Handstein and K. H. Muller, “Influence of the Substrate on Growth and Magnetoresistance of $\text{La}_{0.7}\text{Ca}_{0.3}\text{MnO}_2$ Thin Films Deposited by Magnetron Sputtering,” *Journal of Applied Physics*, Vol. 83, No. 4, 1998, pp. 2152-2157. [doi:10.1063/1.366952](https://doi.org/10.1063/1.366952)
- [15] T. S. Santos, S. J. May, J. L. Robertson and A. Bhattacharya, “Tuning between the Metallic Antiferromagnetic and Ferromagnetic Phases of $\text{La}_{1-x}\text{Sr}_x\text{MnO}_3$ Near $X=0.5$ by Digital Synthesis,” *Physical Review B*, Vol. 80, No. 15, 2009, Article ID: 155114-155120. [doi:10.1103/PhysRevB.80.155114](https://doi.org/10.1103/PhysRevB.80.155114)
- [16] G. H. Therese and P. V. Kamath, “Electrochemical Synthesis of LaMnO_3 Coatings on Conducting Substrates,” *Chemistry of Materials*, Vol.10, No. 11, 1998, pp. 3364-3367. [doi:10.1021/cm980046f](https://doi.org/10.1021/cm980046f)
- [17] H. B. Wang, G. Y. Meng and D. K. Peng, “Aerosol and Plasma Assisted Chemical Vapor Deposition Process for Multicomponent Oxide $\text{La}_{0.8}\text{Sr}_{0.2}\text{MnO}_3$ Thin Film,” *Thin Solid Films*, Vol. 368, No. 2, 2000, pp. 275-278. [doi:10.1016/S0040-6090\(00\)00781-1](https://doi.org/10.1016/S0040-6090(00)00781-1)
- [18] E. H. Walker, A. W. Apblett, R. Walker and A. Zachary, “The Novel Synthesis of $\text{La}_{0.8}\text{Sr}_{0.2}\text{MnO}_3$ Using the Michael-Addition Directed Hydrogelation of Acrylates for Materials Synthesis (MADHAMS) Method,” *Chemical Materials*, Vol. 16, No. 25, 2004, pp. 5336-5343. [doi:10.1021/cm0489385](https://doi.org/10.1021/cm0489385)
- [19] M. G. Harwood, “The Crystal Structure of Lanthanum-Strontium Manganites,” *Proceedings of the Physical Society, Section B*, Vol. 68, No. 9, 1955, pp. 586-590. [doi:10.1088/0370-1301/68/9/302](https://doi.org/10.1088/0370-1301/68/9/302)